AIMS Mathematics, 10(11): 27103–27128.
DOI: 10.3934/math.20251191
Received: 30 July 2025
Revised: 28 October 2025
Accepted: 04 November 2025
Published: 21 November 2025

https://www.aimspress.com/journal/Math

Research article

Fuzzy Gain-Composite approach for robust control of chaotic fractional-order optical systems with guaranteed performance

Sepideh Nikfahm Khoubravan[1], Saeed Mirzajani[2,*], Aghileh Heydari[1] and Majid Roohi[3]

[1] Department of Mathematics, Payame Noor University, Tehran, Iran
[2] Department of Basic sciences, Technical and Vocational University (TVU), Tehran, Iran
[3] Department of Mathematics, Aarhus University, 8000 Aarhus, Denmark

* **Correspondence:** Email: Smirzajani@tvu.ac.ir.

Abstract: In this work, a Guaranteed-Cost Fuzzy Gain-Composite (GC-FGC) control scheme was introduced to stabilize a specialized class of chaotic fractional-order Takagi–Sugeno (T–S) fuzzy nonlinear optical systems. The controller design was grounded in fractional-order Lyapunov theory and formulated using Linear Matrix Inequality (LMI) conditions, enabling the effective handling of the complex chaotic dynamics inherent in such systems. The proposed method ensures asymptotic stability and further incorporates a dynamics-free control strategy that remains robust in the presence of system uncertainties and input saturation constraints. To decouple the control rules from the specific system dynamics, the design leverages the norm-bounded nature of the chaotic system states. Furthermore, a deep reinforcement learning framework based on the Soft Actor-Critic (SAC) algorithm was employed to fine-tune the internal coefficients of the GC-FGC controller. By optimizing a reward function through the SAC agent's neural network, an optimal policy was derived that guarantees finite-time convergence and satisfied the sliding surface reachability conditions. The effectiveness and applicability of the proposed control framework were verified through comprehensive simulations and two illustrative numerical case studies.

Keywords: T-S fuzzy model; fractional-order systems; Guaranteed-cost fuzzy gain-composite control; Lyapunov theory; nonlinear optical systems
Mathematics Subject Classification: 26A33, 37N35, 93C42

1. Introduction

Optical systems are fundamental to numerous technological domains, including precision imaging, optical communication, biomedical instrumentation, and laser-based applications. Many of these systems exhibit complex nonlinear dynamics, especially when modeled in fractional-order domains or when chaos is present, as in high-dimensional laser systems [1]. Accurate control of such systems is essential for maintaining stability, improving performance, and achieving desired operational objectives. However, traditional control techniques often struggle to handle the strong nonlinearities, high-dimensional behavior, and modeling uncertainties inherent in advanced optical platforms [2].

Fractional-order (FO) systems, characterized by differential equations with non-integer order derivatives, have attracted significant interest in recent decades due to their superior ability to model complex dynamics with memory and hereditary properties [3]. Unlike their integer-order counterparts, FO systems offer greater modeling flexibility and accuracy in describing physical phenomena such as viscoelasticity, anomalous diffusion, and electromagnetic behavior [4]. In the field of optics, fractional-order modeling has proven especially valuable for capturing the intrinsic complexity of light-matter interactions and the nonlinear dynamics of advanced optical devices [5].

FO optical systems extend the classical modeling paradigm by incorporating non-integer derivatives, enabling more accurate representation of memory effects, long-range interactions, and anomalous diffusion often observed in real-world optical phenomena. These characteristics make FO models particularly suited for describing hybrid optical systems and chaotic laser dynamics. However, the increased model fidelity comes at the cost of greater mathematical and computational complexity. Such systems often exhibit sensitive dependence on initial conditions, parameter uncertainties, and complex oscillatory behavior, which can lead to instability and degraded performance. Therefore, the development of robust and efficient control strategies for stabilizing FO optical systems is a theoretical and practical necessity, especially in scenarios demanding high precision, speed, and resilience to disturbance [6].

A wide array of control strategies has been developed to tackle the complex behavior of nonlinear and fractional-order systems, including PID control [7,8], sliding mode control [9,10], adaptive control [11], backstepping techniques [12], and intelligent methods such as fuzzy logic control [13,14] and artificial neural networks [15,16]. These approaches have demonstrated varying degrees of success in stabilizing optical and chaotic systems, especially under modeling uncertainty and external disturbances. However, their effectiveness can be limited when dealing with highly nonlinear or high-dimensional systems, particularly those exhibiting fractional-order dynamics.

In this context, the Takagi–Sugeno (T–S) fuzzy modeling framework offers a promising alternative for handling system nonlinearity. By decomposing a nonlinear system into a convex combination of linear subsystems using fuzzy membership functions, the T–S approach enables systematic controller design through linear matrix inequalities (LMIs) [17]. This structure facilitates the application of rigorous mathematical tools for stability analysis and control synthesis, making it particularly useful for optical systems with complex, uncertain dynamics.

The authors of [18] use a membership-function-dependent fuzzy Lyapunov function and a new fractional derivative rule to analyze stability and design controllers for fractional-order T–S fuzzy systems. In [19], an observer-based adaptive robust control is proposed for FO TS fuzzy systems with input uncertainties and output disturbances, using an augmented fuzzy model and LMI-based stability

analysis. In [20], a fuzzy FO unknown input observer is designed for fault estimation in nonlinear FO systems using the TS fuzzy model. The method decouples unknown inputs and uses LMIs with fuzzy Lyapunov functions to ensure observer stability. The authors of [21] propose an adaptive control method for fractional-order T–S fuzzy systems with time delays, unknown parameters, and input saturation, using an auxiliary system and norm conversion to ensure stability and boundedness.

An event-triggered integral sliding mode controller is designed for fractional-order T–S fuzzy systems using a fuzzy error function and a mixed time-varying/fixed threshold to ensure stability and reduce control updates, as done by the authors of [22]. In [23], an output feedback tracking control and disturbance rejection method was developed for nonlinear fractional-order systems using a T–S fuzzy model and a fractional-order modified repetitive controller, with stability ensured by a fuzzy Lyapunov function and LMIs. In [24], an uncertainty and disturbance estimator-based tracking control method was developed for interval type-2 fractional-order T–S fuzzy systems with time-varying delays, ensuring stability and accurate estimation without prior knowledge of uncertainties, as done by the authors. The authors of [25] designed a region-bounded observer for T–S fuzzy systems using a membership-dependent Lyapunov–Krasovskii functional and LMI-based conditions, addressing disturbances and noise. In [26], an adaptive T–S fuzzy control scheme was proposed for synchronizing uncertain fractional-order chaotic systems with input saturation and disturbances, using FO adaptive laws and avoiding LMI computations, as done by the authors. In [27], an event-triggered controller was proposed for finite-time stabilization of T–S fuzzy systems with time-scale delays, using LMI-based criteria without relying on delayed state feedback. The authors of [26] proposed an adaptive T–S fuzzy controller for uncertain fractional-order chaotic systems with input saturation, avoiding LMIs and ensuring asymptotic synchronization via FO adaptive laws. In [28], an adaptive fuzzy control method based on Q-learning was proposed for fractional-order nonautonomous systems with input delay and faults, using fuzzy observers and Lyapunov-based stability analysis within an actor–critic framework, as done by the authors. In [29], an optimal fractional-order sliding mode controller was designed using the T–S fuzzy model and actor–critic reinforcement learning to ensure stability and reduce chattering in FO systems.

However, despite the notable advancements in the above studies, several limitations remain that restrict their practical applicability and robustness, particularly in complex fractional-order systems such as chaotic or optical dynamics. These include:

I. Most researchers focus on stability or synchronization but do not provide a *guaranteed-cost* framework, meaning they lack formal control over the worst-case performance (energy, tracking error, etc.).
II. Several methods rely extensively on solving complex sets of LMIs, especially those using fuzzy Lyapunov or Krasovskii functionals, which can be computationally intensive and less scalable to higher-order systems.
III. Input saturation and system constraints are addressed only in a few works and often with approximations or conservative assumptions that may limit practical applicability.
IV. Most controllers use fixed design parameters or adaptive rules derived analytically. They do not leverage data-driven or learning-based techniques (e.g., deep reinforcement learning) to fine-tune gains for enhanced performance.
V. While some works target fractional-order or chaotic systems, very few address optical systems or complex hybrid fractional-order optical chaos, which present unique challenges in terms of dimensionality and sensitivity.

VI. Several papers emphasize observer or estimation design (e.g., FFOPIO, region-bounded observers), but do not propose comprehensive controller designs for stabilization or synchronization under uncertainties.

Despite the progress achieved in existing studies, the literature lacks a comprehensive framework that explicitly integrates guaranteed-cost control with fuzzy gain-composite design for fractional-order optical systems. Most researchers have primarily focused on stability or synchronization without providing an explicit formulation of cost performance under uncertainty and input saturation. Furthermore, the incorporation of adaptive learning mechanisms, such as the SAC algorithm, within the T–S fuzzy framework remains largely unexplored, particularly for complex optical systems characterized by fractional-order dynamics and high sensitivity to initial conditions.

The major contributions of this paper can be summarized as follows:

I. A Guaranteed-Cost Fuzzy Gain-Composite control framework is developed for fractional-order nonlinear optical systems, ensuring robust stability and bounded performance under parameter uncertainties and input constraints.

II. The proposed approach explicitly integrates Guaranteed-Cost control with Takagi–Sugeno fuzzy modeling, enabling systematic controller design while providing formal performance guarantees; an aspect not addressed in prior fuzzy control studies.

III. The controller effectively handles actuator saturation and input constraints through a gain-composite design, enhancing practical applicability and robustness.

IV. A Deep Reinforcement Learning mechanism (Soft Actor–Critic) is employed to adaptively tune fuzzy gain parameters, improving convergence speed and adaptability in dynamic environments while maintaining guaranteed-cost performance.

V. The framework is specifically tailored for complex fractional-order chaotic optical systems, which have rarely been explored in guaranteed-cost or fuzzy control studies.

VI. Comparative simulations validate the proposed method, demonstrating superior stability, convergence, and disturbance rejection compared to conventional fuzzy and guaranteed-cost controllers.

The remainder of this article is organized as follows. In Section 2, some necessary definitions of fractional-order calculus and preliminaries for T-S fuzzy modeling of nonlinear systems are given and descriptions the system are provided. The proposed GC-FGC controller is designed in Section 3. A Deep Reinforcement Learning (SAC) mechanism is incorporated for adaptive tuning of fuzzy gain parameters, enhancing convergence and adaptability; this aspect is detailed in Section 4. Numerical computer simulations are presented in Section 5. Finally, this paper ends with concluding remarks in Section 6.

2. Preliminaries and system description

In this section, we introduce essential definitions related to fractional-order systems and present fundamental criteria used in the analysis of their stability. Additionally, key concepts of T-S fuzzy modeling are reviewed to facilitate the representation and control of nonlinear FO systems through rule-based linear approximations.

Our main control objective of this study is to design a Guaranteed-Cost Fuzzy Gain-Composite (GC-FGC) controller capable of stabilizing fractional-order nonlinear optical systems under parameter uncertainties, external disturbances, and input constraints. The proposed framework ensures

asymptotic stability and guarantees an upper bound on the performance cost while maintaining robustness and adaptability through the integration of deep reinforcement learning. The subsequent sections are organized to present the mathematical preliminaries, the proposed control design, and numerical validations in a clear and coherent manner.

2.1. Basic concepts and stability requirements of fractional-order systems

In this part, we introduce essential definitions related to FO systems and present fundamental criteria used in the analysis of their stability.

Definition 1. The fractional-order Riemann-Liouville integral of order α for a function is defined by [30]:

$$ {}_{t_0}I_t^{\alpha}\Upsilon(t) = {}_{t_0}D_t^{-\alpha}\Upsilon(t) = \frac{1}{\Gamma(\alpha)}\int_{t_0}^{t}\frac{\Upsilon(\theta)}{(t-\theta)^{1-\alpha}}d\theta \tag{2.1} $$

where t_0 is the initial moment, α is a positive real number indicating the integration order, and $\Gamma(\cdot)$ stands for the Gamma function, which is defined by $\Gamma(\psi) = \int_{t_0}^{\infty} e^{-\theta}t^{\psi-1}d\theta$.

Definition 2. The Caputo fractional derivative of order $\alpha \in R^{+}$for a function $g(t)$is defined as [30]:

$$ D^{\alpha}g(t) = \frac{1}{\Gamma(n-\alpha)}\int_{a}^{t}\frac{g^{(n)}(\theta)}{(t-\theta)^{\alpha-n+1}}d\theta \tag{2.2} $$

where $n = min\{k \in N, k > \alpha\}$.

Using this definition, an uncertain fractional-order system with control input can be modeled as:

$$ D^{\alpha}x(t) = g(x, t, \Delta, u), \tag{2.3} $$

where $\alpha \in (0,1)$, x denotes the system states, t is the time variable, Δ represents the system uncertainties, and u corresponds to the control input.

Remark 1. The Caputo fractional-order derivative is employed in model (2.2) due to its practical advantages for modeling and control of physical systems. Unlike the Riemann–Liouville (R–L) derivative, the Caputo formulation allows the use of standard initial conditions defined in terms of integer-order derivatives, simplifying implementation and numerical simulations. Furthermore, it provides a flexible framework to capture memory and hereditary effects in complex dynamical systems, effectively representing nonlocal and history-dependent behaviors. These properties make it particularly suitable for control and stability analysis of fractional-order systems. Moreover, under standard assumptions, the qualitative dynamic behavior of the system remains similar if the R–L derivative is adopted, and the proposed control strategy can be adapted with minor modifications. The Caputo derivative also enables a straightforward extension of classical control techniques to the fractional-order domain, maintaining compatibility with standard initial-value problems [31–33].

Proposition 1 [34]: For $r-1 < \alpha < r \in Z^{+}$ and $y(t) \in C^{m}[0,T]$, then

$$ D^{-\beta}\left(D^{\beta}y(t)\right) = y(t) - \sum_{k=0}^{n-1}\frac{t^k}{k!}y(0). \tag{2.4} $$

From (2.4), if $\alpha \in (0,1)$ and $g(t) \in C^{m}[0,T]$, in that case

$$ D^{-\alpha}\left(D^{\alpha}g(t)\right) = g(t) - g(0). \tag{2.5} $$

Lemma 1: Consider real matrices X, Y, and $\Xi(t)$ of compatible dimensions, where the matrix $\Xi(t)$ satisfies the condition $\Xi^T(t) \cdot \Xi(t) \leq I$. Under this assumption, the following inequality holds:

$$\pm X\Xi(t)Y \pm X^T\Xi^T(t)Y^T \leq \varepsilon XX^T + \varepsilon^{-1}Y^TY. \tag{2.6}$$

This inequality holds true for every positive scalar $\varepsilon > 0$.

Proof. See Appendix A.

Remark 2. Let X and Y be real matrices of compatible dimensions. Then, the following inequality holds:

$$X^TY + Y^TX \leq \frac{X^T\pi X}{\varepsilon} + \varepsilon Y^T\pi^{-1}Y \leq \frac{X^T\pi X}{\varepsilon} + \varepsilon\frac{Y^TY}{\lambda(\pi)_{min}}, \tag{2.7}$$

where $\varepsilon > 0$ is a scalar, and $\lambda(\cdot)_{min}$ denotes the minimum eigenvalue of the matrix.

Theorem 1. Consider the non-autonomous fractional-order system [35]:

$$D^\alpha x(t) = g(x,t), \tag{2.8}$$

where $x = 0$ is an equilibrium point, $g(x,t)$ satisfies the Lipschitz condition with constant $l > 0$, and the order $\alpha \in [0,1]$. Suppose there exists a Lyapunov function $V\big(t, x(t)\big)$ along with class-K functions Υ_i for $i = 1,2,3$, such that:

$$\Upsilon_1(\|x\|) \leq V(x(t),t) \leq \Upsilon_2(\|x\|), \tag{2.9}$$

$$D^\alpha V(x(t),t) \leq -\Upsilon_3(\|x\|), \tag{2.10}$$

then the equilibrium points $x = 0$ of system (8) is asymptotically stable.

2.2. Generalized T-S fuzzy model of fractional-order systems

In this section, we formulate the control problem for uncertain fractional-order systems represented by T-S fuzzy models.

Assume that the nonlinear, non-autonomous system described in equation (2.3), which includes uncertainties and control inputs, can be approximated using a Fractional-Order T-S Fuzzy Model (FOTSFM) as follows:

Model Rule i:

If $z_1(t)$ is M_{i1}, and $z_2(t)$ is M_{i2}, ..., and $z_p(t)$ is M_{ip}, then

$$D^\alpha x_i(t) = (A_i + \Delta A_i)x(t) + B_iu(t) \qquad i = 1,\dots,r. \tag{2.11}$$

Here, M_{ij} for $(j = 1\dots p)$ represents fuzzy sets associated with the premise variables, r denotes the total number of fuzzy IF–THEN rules, and $x(t) \in R^n$ is the system state vector. The matrices $A_i \in R^{n\times n}$ define the local system dynamics, while $z_1(t), \dots, z_p(t)$ are the premise variables. Parameter $\alpha \in (0,1)$ indicates the fractional order of the system.

The overall output of the generalized T-S fuzzy model is derived through a fuzzy inference mechanism as follows:

$$D^\alpha x(t) = \frac{\sum_{i=1}^r w_i\big(z(t)\big)\cdot\{(A_i+\Delta A_i)x(t)+B_iu(t)\}}{\sum_{i=1}^r w_iz(t)} \tag{2.12}$$

In the expression above, the vector $z(t) = \left(z_1(t), \ldots, z_p(t)\right)$ contains the premise variables, and the weighting function for the i-th rule is defined as $w_i\big(z(t)\big) = \prod_{j=1}^{p} M_{ij}\left(z_j(t)\right)$, where $M_{ij}\left(z_j(t)\right)$ denotes the membership degree of $z_j(t)$ in the fuzzy set M_{ij}. These membership functions satisfy the following conditions:

$$\begin{aligned} &\textstyle\sum_{i=1}^{r} w_i\big(z(t)\big) > 0, \\ &w_i\big(z(t)\big) \geq 0. \end{aligned} \tag{2.13}$$

By introducing normalized weights defined as $h_i\big(z(t)\big) = \frac{w_i(z(t))}{\sum_{i=1}^{r} w_i(z(t))}$, expression (2.13) can be reformulated accordingly as:

$$D^{\alpha} x_i(t) = \textstyle\sum_{i=1}^{r} h_i\left(z(t)\right) \cdot \{(A_i + \Delta A_i)x(t) + B_i u(t)\}, \tag{2.14}$$

In addition, the following conditions must be satisfied:

$$\begin{cases} \sum_{i=1}^{r} h_i\left(z(t)\right) = 1, \\ h_i\big(z(t)\big) \geq 0. \end{cases} \tag{2.15}$$

The terms $h_i\big(z(t)\big)$ represent the normalized weighting factors associated with each IF–THEN rule.

3. System demonstration and problem statement

In this section, we focus on the design of a non-fragile control framework based on T–S fuzzy techniques for nonlinear uncertain fractional-order systems.

3.1. System description

Consider the following n-dimensional fractional-order nonlinear system subject to model uncertainties and external disturbances:

$$D^{\alpha} x_i(t) = (A_i + \Delta A_i)x(t) + B_i u(t), \tag{3.1}$$

where $\alpha \in (0,1)$ denotes the fractional order, $x(t) = [x_1(t), \ldots, x_n(t)]^T \in \mathbb{R}^n$ is the state vector, ΔA_i represents unknown system uncertainties, B_i shows the input-gain-function of the system, and $u(t) = [u_1(t), \ldots, u_n(t)]^T \in \mathbb{R}^n$ is the control input.

Assuming nonlinear non-autonomous system (3.1) can be represented by a FO TS Fuzzy, the model rule i is described as follows:

Model Rule i:

If $z_1(t)$ is M_{i1},…,and $z_p(t)$ is M_{ip},Then

$$D^{\alpha} x_i(t) = \textstyle\sum_{i=1}^{r} h_i\left(z(t)\right) \cdot \{(A_i + \Delta A_i)x(t) + B_i u(t)\}, \tag{3.2}$$

where $x(t) \in \mathbb{R}^n$ is the state vector of the nonlinear system $z(t) = \left[z_1(t), \ldots, z_p(t)\right]^T$ denotes the

premise variables, M_{ij} (for $j = 1, \ldots, p$ and $i = 1, \ldots, r$) are fuzzy sets, and r is the total number of fuzzy rules. The matrices A_i and B_i have compatible dimensions, and, ΔA_i corresponds to the system's unknown parameter uncertainties.

To establish the major results, we begin by defining the cost function associated with system (2.3) as follows:

$$D^{-\alpha} = \int_0^{\infty} [x^T(s) \cdot Q \cdot x(s) + u^T(s) \cdot R \cdot u(s)]\, ds, \tag{3.3}$$

where Q and R are given positive definite symmetric matrices.

Corresponding to the cost function (3.3), the fuzzy guaranteed cost control is defined as:

Definition 3. For the T–S fuzzy system described by (3.2), if there exists a control input $u(t)$ and a positive scalar J^*such that the closed-loop system is stable and the cost function satisfies $J \leq J^*$, then J^* is referred to as the guaranteed cost, and $u(t)$ is called the guaranteed cost control law for the T–S fuzzy system (3.2).

3.2. System description

To achieve global asymptotic stabilization of the origin for the system described in (3.3), a fuzzy guaranteed cost control strategy based on state feedback is proposed as follows:

Control Rule j:

If $z_1(t)$ is M_{j1},…, and $z_r(t)$ is M_{jr} , Then

$$u(t) = -K_j L_j x(t), \tag{3.4}$$

where $K_j \in \mathbb{R}^{r \times n}$ are state composites gain matrices of appropriate dimensions.

To allow for possible dynamic weighting in the control structure, define the matrix $L_j = diag\left(L_1^j, \ldots, L_r^j\right)$, where $L_i^j \in \{0,1\}$ acts as a binary scaling or enabling factor. When $L_i^j = 1$, the corresponding controller component is active; when $L_i^j = 0$, it is deactivated.

Thus, the Guaranteed-Cost Fuzzy Gain-Composite control law is given by:

$$u(t) = -\sum_{j=1}^{m} h_j\big(z(t)\big) L_j K_j\, x(t), \quad t \geq 0. \tag{3.5}$$

where $h_j\big(z(t)\big)$ are the normalized membership functions associated with the fuzzy rules.

Before deriving the main theorem for determining the control gains $L_j K_j$ a supporting lemma is introduced.

Lemma 2 [36]: (Schur complement).

Let $S = \begin{pmatrix} s_{11} & s_{12} \\ s_{21} & s_{22} \end{pmatrix}$ be a symmetric matrix such that $s_{11} = s_{11}^T$, and $s_{22} = s_{22}^T$. Then, the following two statements are equivalent:

(1) $S < 0$ (i.e., the matrix S is negative definite);

(2) $s_{22} < 0, s_{11} - s_{12} s_{22}^{-1} s_{12}^T < 0$.

In the following, an asymptotic stability condition is established for nonlinear systems modeled using T-S fuzzy frameworks.

Theorem 2. Consider the fractional-order system defined in (3.2). If there exist symmetric positive definite matrices $\hat{P}$ and controller gain matrices $\hat{K}_j, \hat{L}_j$ for all $j \in \{1, \ldots, m\}$ such that the following LMI holds for every $i, j \in \{1, \ldots, m\}$:

$$\tilde{\psi}_{ij} = \begin{pmatrix} A_i\hat{P} + \hat{P}A_i^T + \Delta A_i\hat{P} + \hat{P}\Delta A_i^T - B_i\hat{K}_j\hat{L}_j - \hat{K}_j^T\hat{L}_j^T B_i^T & \hat{P} & \hat{K}_j^T\hat{L}_j^T \\ * & -Q^{-1} & 0 \\ * & * & -R^{-1} \end{pmatrix} < 0, \tag{3.6}$$

then system (3.2) can be asymptotically stabilized by the state feedback controller given in (3.5). The resulting stabilizing gain is computed as: $K_j = \hat{K}_j\hat{P}^{-1}$.

Furthermore, the cost function defined in (3.3) satisfies the following upper bound:

$$J \le J^* = x^T(0)Px(0),$$

where $P = \hat{P}^{-1}$. This ensures that the system is stabilized with a guaranteed performance bound.

$J \le J^* = x^T(0)Px(0)$.

where $P = \hat{P}^{-1}$, and non-fragile tolerant control of fractional systems is obtained.

The stabilizing gain K_j is obtained by first solving the LMI condition above to determine the auxiliary matrices $\hat{K}_j$and the positive definite matrix $\hat{P}$. The final gain is then recovered via $K_j = \hat{K}_j\hat{P}^{-1}$. This approach ensures that the closed-loop system is asymptotically stable while maintaining a guaranteed upper bound on the performance index $J \le J^*$, even in the presence of modeling uncertainties and external disturbances. This explicit derivation highlights the connection between the LMI-based design and the resulting guaranteed-cost control performance, providing a clear and practical procedure for controller synthesis.

Proof. Consider the following Lyapunov function candidate for the system:

$$V\big(x(t)\big) = x^T(t) \cdot P \cdot x(t), \;\; P = \hat{P}^{-1} > 0. \tag{3.7}$$

Using the Caputo derivative for $0 < \alpha < 1$, the derivative of the Lyapunov function along trajectories of the system becomes:

$$D^\alpha V\big(x(t)\big) = D^\alpha(x^T Px) \le 2x^T(t)PD^\alpha x(t), \tag{3.8}$$

Substituting the closed-loop dynamics of the fractional-order T-S fuzzy system (3.2) under the controller (3.5), we obtain $D^\alpha x(t) = \sum_{i=1}^r h_i\big(z(t)\big) \cdot \{(A_i + \Delta A_i)x(t) + B_i u(t)\}$ and $u(t) = -\sum_{j=1}^m h_j\big(z(t)\big)L_jK_j\,x(t)$. Hence,

$$D^\alpha V\big(x(t)\big) \le 2\sum_{i=1}^r\sum_{j=1}^m h_i\big(z(t)\big)h_j\big(z(t)\big)x^T(t)P\big(A_i + \Delta A_i - B_iL_jK_j\big)\,x(t). \tag{3.9}$$

Using the symmetry of the Lyapunov function, we define:

$$\Phi_{ij} = P\big(A_i + \Delta A_i - B_iL_jK_j\big) + \big(A_i + \Delta A_i - B_iL_jK_j\big)^T P. \tag{3.10}$$

By defining the symmetric matrix Φ_{ij}, the factor of 2 in (3.9) is absorbed, and the Lyapunov derivative can be equivalently expressed in terms of Φ_{ij}. Using the convex combination property of the fuzzy weights $h_i(z(t))$ and $h_j(z(t))$, the derivative is then rewritten as the double summation in (3.11), providing a concise quadratic form representation without explicitly carrying the factor 2.

which leads to:

$$D^\alpha V\big(x(t)\big) \le \sum_{i=1}^r\sum_{j=1}^m h_i\,h_j x^T(t)\Phi_{ij}\,x(t). \tag{3.11}$$

Now, considering the cost function:

$$J = D^{-\alpha}[x^T(t) \cdot Q \cdot x(t) + u^T(t) \cdot R \cdot u(t)], \tag{3.12}$$

and substituting the control input, we obtain:

$$u(t) = -L_j K_j x(t) \Rightarrow u^T(t) \cdot R \cdot u(t) \ = x^T(t) {K_j}^T {L_j}^T R L_j K_j x(t).$$

Therefore, we construct the following dissipation inequality:

$$D^{\alpha} V\big(x(t)\big) + x^T(t) \cdot Q \cdot x(t) + u^T(t) \cdot R \cdot u(t)$$

$$\leq \sum_{i=1}^{r} \sum_{j=1}^{m} h_i \, h_j x^T(t) \big(\Phi_{ij} + Q + {K_j}^T {L_j}^T R L_j K_j\big) x(t). \tag{3.13}$$

To handle the uncertain term ΔA_i, we apply **Remark 2**, which provides the bound:

$$P\Delta A_i + \Delta {A_i}^T P \leq \frac{1}{\varepsilon} \mathrm{P}\Pi\mathrm{P} + \varepsilon \Delta {A_i}^T \Pi^{-1} \Delta A_i,$$

for $\varepsilon > 0$ and positive definite matrix Π, enabling quadratic bounding of uncertainties. Incorporating this into the matrix inequality and applying **Lemma 2** (Schur complement), we conclude that the condition:

$$\tilde{\psi}_{ij} = \begin{pmatrix} A_i \hat{P} + \hat{P} A_i^T + \Delta A_i \hat{P} + \hat{P} \Delta A_i^T - B_i \hat{K}_j \hat{L}_j - \hat{K}_j^T \hat{L}_j^T B_i^T & \hat{P} & \hat{K}_j^T \hat{L}_j^T \\ * & -Q^{-1} & 0 \\ * & * & -R^{-1} \end{pmatrix} < 0. \tag{3.14}$$

By applying Lemma 2 (Schur complement) to the LMI in (3.14) and incorporating the bound on the uncertain term ΔA_i from **Remark 2**, we can transform the matrix inequality into a scalar dissipation inequality along the system trajectories. This ensures that

$$D^{\alpha} V\big(x(t)\big) + x^T(t) \cdot Q \cdot x(t) + u^T(t) \cdot R \cdot u(t) < 0. \tag{3.15}$$

as stated in (3.15). This step formally links the LMI condition to the Lyapunov derivative and guarantees that the closed-loop system satisfies the desired stability and performance properties.
Therefore, from the inequality (3.15), $D^{\alpha} V\big(x(t)\big) < 0$. We conclude that system (3.3) with (3.4) is asymptotically stable.

Now, by taking fractional order integrating of (3.15) from 0 to ∞, one has

$$D^{-\alpha} \Big(D^{\alpha} V\big(x(t)\big) + x^T(t) \cdot Q \cdot x(t) + u^T(t) \cdot R \cdot u(t) \Big) < 0. \tag{3.16}$$

Using (2.5) in relation (3.16), one obtains

$$V\big(x(t)\big) - V\big(x(0)\big) + D^{-\alpha} \big(x^T(t) \cdot Q \cdot x(t) + u^T(t) \cdot R \cdot u(t) \big) < 0 \tag{3.17}$$

Therefore,

$$V\big(x(t)\big) + D^{-\alpha} \big(x^T(t) \cdot Q \cdot x(t) + u^T(t) \cdot R \cdot u(t) \big) < V\big(x(0)\big). \tag{3.18}$$

Since

$$D^{-\alpha}\left(x^T(t)\cdot Q\cdot x(t)+u^T(t)\cdot R\cdot u(t)\right)<V\left(x(0)\right)=x^T(0)\cdot P\cdot x(0). \tag{3.19}$$

which implies that the system is asymptotically stable, and the performance index is bounded above by $J\leq J^*=x^T(0)Px(0)$. Finally, the control gain is recovered by $K_j=\widehat{K}_j\hat{P}^{-1}$, ensuring that the controller stabilizes the system and achieves guaranteed performance despite uncertainties.

Remark 3. The fractional order $\alpha\in(0,1)$ introduces memory and hereditary properties into the system, meaning the future evolution depends not only on the current state but also on past states. Intuitively, this "memory effect" slows the system dynamics and smooths transient responses, which can enhance robustness against disturbances. However, this also affects the LMI-based controller design: Smaller values of α generally impose stricter feasibility conditions on the LMIs, requiring more conservative solutions to guarantee asymptotic stability. Conversely, as α approaches 1, the system behaves more like an integer-order system, and the LMI constraints become less restrictive. Therefore, the choice of α directly impacts the controller conservatism and the achievable performance bounds.

Remark 4. The primary objective of the proposed GC-FGC controller is to asymptotically stabilize fractional-order nonlinear optical systems while ensuring an upper bound on the performance cost. The framework effectively addresses parameter uncertainties, external disturbances, and input constraints. Through the integration of deep reinforcement learning, the controller adaptively fine-tunes its internal parameters, enhancing robustness, convergence speed, and overall performance.

Remark 5. The GC-FGC controller, designed and theoretically analyzed in Section 3, provides formal stability guarantees and performance bounds under uncertainties and input constraints. However, the controller's performance critically depends on the selection of internal gain parameters $\{K_i, L_i, Q, R\}$. To enhance adaptability and convergence, Section 4 incorporates the SAC algorithm, which continuously updates these parameters based on real-time system states. Specifically, the actor network proposes adjustments to the control gains, while the critic network evaluates the resulting cumulative reward to refine the parameters iteratively. This learning-assisted mechanism ensures that the GC-FGC controller not only maintains guaranteed-cost performance but also dynamically adapts to changing operating conditions, disturbances, and model uncertainties, effectively bridging the theoretical design with practical implementation.

4. Set up of Adaptive TS Fuzzy controller using Deep SAC learning

4.1. Fundamental concepts of MDP and reinforcement learning algorithms

In practical scenarios, the agent may not have full access to all the system's states, which motivates the use of Markov Decision Process (MDP) modeling. MDPs provide a structured approach to represent the system's dynamics, enabling the agent's policy to be designed based on the system's intrinsic behavior. As defined, an MDP assumes that the next state of the environment depends solely on the current state, following the Markov property [37]. Conventionally, an MDP is characterized by a five-element tuple $\langle \mathcal{L}, \mathcal{B}, \mathcal{P}, \beth, \gimel \rangle$, defined as follows:

- $\wp \in \mathcal{L}$ represents the set of system states (observations).
- $w \in \mathcal{B}$ denotes the set of available actions.

- The transition function $\mathcal{P}: \mathcal{L} \times \mathcal{B} \times \mathcal{L} \to [0,1)$ defines the probability of moving from the current observation $\wp_t$ the next observation $\wp_{t+1}$, given that action w_t is taken.
- The reward function $ב \in \mathcal{L} \times \mathcal{B} \to \mathcal{R}$ generates scalar feedback from the environment in response to the action w_t taken by the agent.
- A history $\hbar_t = (\wp_0, w_1, \ldots, w_{t-1}, \wp_t)$ maintains the complete sequence of observations and corresponding actions up to time.

At each time step, the reinforcement learning agent interacts with the environment based on the current observation $\wp_t$ triggering a reward $ב_t$. To determine the next action, a policy $\varphi(w|\wp)$ is employed, which governs the decision-making behavior of the agent.

In reinforcement learning tasks, the objective of the agent is to maximize the cumulative discounted reward, defined as:

$$G_t = ב_{t+1} + ג ב_{t+2} + \cdots = \sum_{k=0}^{\infty} ג^k ב_{t+k+1}, \tag{4.1}$$

To facilitate this objective, two key functions are introduced: The state-value function $V_\varphi(\wp)$, and the action-value function $\mathcal{Q}_\varphi(\wp, w)$, which are formally defined in Eqs (4.2) and (4.3), respectively.

$$V_\varphi(\wp) = \mathbb{E}_\varphi[G_t|\mathcal{L}_t = \wp], \tag{4.2}$$

$$\mathcal{Q}_\varphi(\wp, w) = \mathbb{E}_\varphi[G_t|\mathcal{L}_t = \wp, \mathcal{B}_t = w], \tag{4.3}$$

4.2. The SAC algorithm

SAC algorithm is a reinforcement learning technique designed to handle complex, high-dimensional environments by leveraging the representation power of deep neural networks (DNNs). A key feature of SAC is the incorporation of entropy regularization, which encourages the policy to maintain a trade-off between maximizing cumulative rewards and promoting sufficient randomness in action selection. This entropy-aware policy framework helps avoid early convergence to suboptimal solutions and enhances the agent's exploration behavior. The learning process in SAC involves optimizing the reward signal and the entropy term concurrently [35,36].

$$J(\varphi) = \sum_{t=0}^{T} \mathbb{E}_{(\wp_t, w_t)\sim\rho_\pi} \left[ב_t(\wp_t, w_t) + \beta\mathcal{H}\left(\varphi(\cdot\,|\wp_t)\right)\right]. \tag{4.4}$$

Here, β is a tunable hyperparameter that regulates the contribution of entropy in the learning objective. The SAC framework comprises three primary deep neural networks: A Q-network, a value network (V-net) and a policy network. Additionally, a replay buffer is employed to retain past state transitions, which are sampled during training to enhance learning stability.

The Q-network, with parameters denoted by θ, is updated by minimizing a soft version of the Bellman equation, expressed as:

$$J_Q(\theta) = \mathbb{E}_{(\wp_t, w_t)\sim D}\left[\frac{1}{2}\left(\mathcal{Q}_\theta(\wp_t, w_t) - \hat{\mathcal{Q}}(\wp_t, w_t)\right)^2\right]. \tag{4.5}$$

In which

$$\hat{Q}(\wp_t, w_t) = \beth(\wp_t, w_t) + \gimel \mathbb{E}_{\wp_{t+1}\sim\rho_\pi}\left[V_{\bar{\emptyset}}(\wp_{t+1})\right]. \tag{4.6}$$

In this context, $V_{\bar{\emptyset}}$ denotes the output of the value network, parameterized by $\emptyset$, which is used to compute gradients during training.
The value function V is formulated as follows:

$$J_V(\emptyset) = \mathbb{E}_{\wp_t\sim D}\left[\frac{1}{2}\left(J_V(\wp_t) - \mathbb{E}_{\wp_t\sim\pi}[Q_\theta(w_t, \wp_t)] - log\varphi(w_t|\wp_t)\right)^2\right]. \tag{4.7}$$

Here, D represents the data distribution drawn from the experience replay buffer.
The policy network, with parameters denoted by ϖ, is optimized using the following objective:

$$J_\varphi(\varpi) = \mathbb{E}_{\wp_t\sim D}\left(D_{KL}\left(\varphi(\cdot\,|\wp_t)\|\frac{exp(Q_\theta(\wp_t,\cdot))}{Z_\theta(\wp_t)}\right)\right). \tag{4.8}$$

Additionally, the SAC algorithm employs two auxiliary networks: A target Q-network and a target policy network. These networks are updated gradually using soft update techniques derived from the corresponding primary networks.

4.3. Guaranteed-Cost Fuzzy Gain-Composite controller design using SAC

The performance of TS Fuzzy Control is highly sensitive to the choice of its internal parameters. To address this, the proposed method employs the SAC algorithm to dynamically tune the coefficients embedded within the Adaptive TS Fuzzy Control law. In this framework, the actor network produces adaptive adjustment signals that continuously refine the control parameters, thereby enhancing system performance.

The set of composite gain parameters to be optimized is denoted by $\Xi = \{K_i,\ L_i,\ Q, R\}$, which are adaptively regulated by the deep reinforcement learning mechanism of SAC. The overall structure of the proposed Adaptive TS Fuzzy Control system enhanced by SAC is illustrated in Figure 1.

Leveraging the training capabilities of deep neural networks, actor and critic networks are optimized to maximize the cumulative reward. The reward function is defined as follows:

$$\beth = \frac{1}{|x|}, \tag{4.9}$$

The reward function in (4.9) is chosen to directly incentivize the minimization of the system state deviation. By assigning higher rewards to smaller values of $|\ x\ |$, the SAC algorithm encourages the controller to reduce the tracking error and stabilize the system more effectively. This design ensures that the learning process focuses on achieving accurate state regulation while maintaining guaranteed cost performance.

The deep neural networks used in the SAC framework, including the Q-network, value network, policy network, and their corresponding target networks, are structured with two hidden layers containing 200 and 300 neurons, respectively. Rectified Linear Units (ReLU) are employed as activation functions within these layers. All three networks are trained using the ADAM optimization algorithm. The specific hyperparameter settings for the deep SAC model are summarized in Table 1.

Remark 6. For better readability, the major symbols used in this section are clarified as follows: $\wp$

denotes the system state (observation), w the control action, P the transition probability function, $\mathcal{R}$ the reward, and $\phi(\cdot|\wp)$ the stochastic policy. The parameters $\theta, \emptyset, \varpi$ correspond to the Q-network, value-network, and policy-network, respectively. The composite fuzzy gain set is defined as $\Xi = \{K_i, L_i, Q, R\}$, which is adaptively tuned by the SAC mechanism. Moreover, γ represents the reward discount factor, β the entropy coefficient in the SAC objective, and x the system state vector used in the reward function.

Remark 7. The SAC algorithm is employed to adaptively tune the internal control parameters $\Xi = \{K_i, L_i, Q, R\}$ of the proposed TS fuzzy gain-composite controller. At each control step, the actor network generates parameter adjustment signals based on the current system state, while the critic network evaluates the expected cumulative reward associated with these parameters. By maximizing the reward function, SAC iteratively updates the control gains, improving convergence, robustness, and performance. This learning-assisted mechanism is fully integrated into the control loop: The SAC outputs directly modify the fuzzy gain parameters used in the controller, thereby ensuring that the system adapts to uncertainties and disturbances in real time.

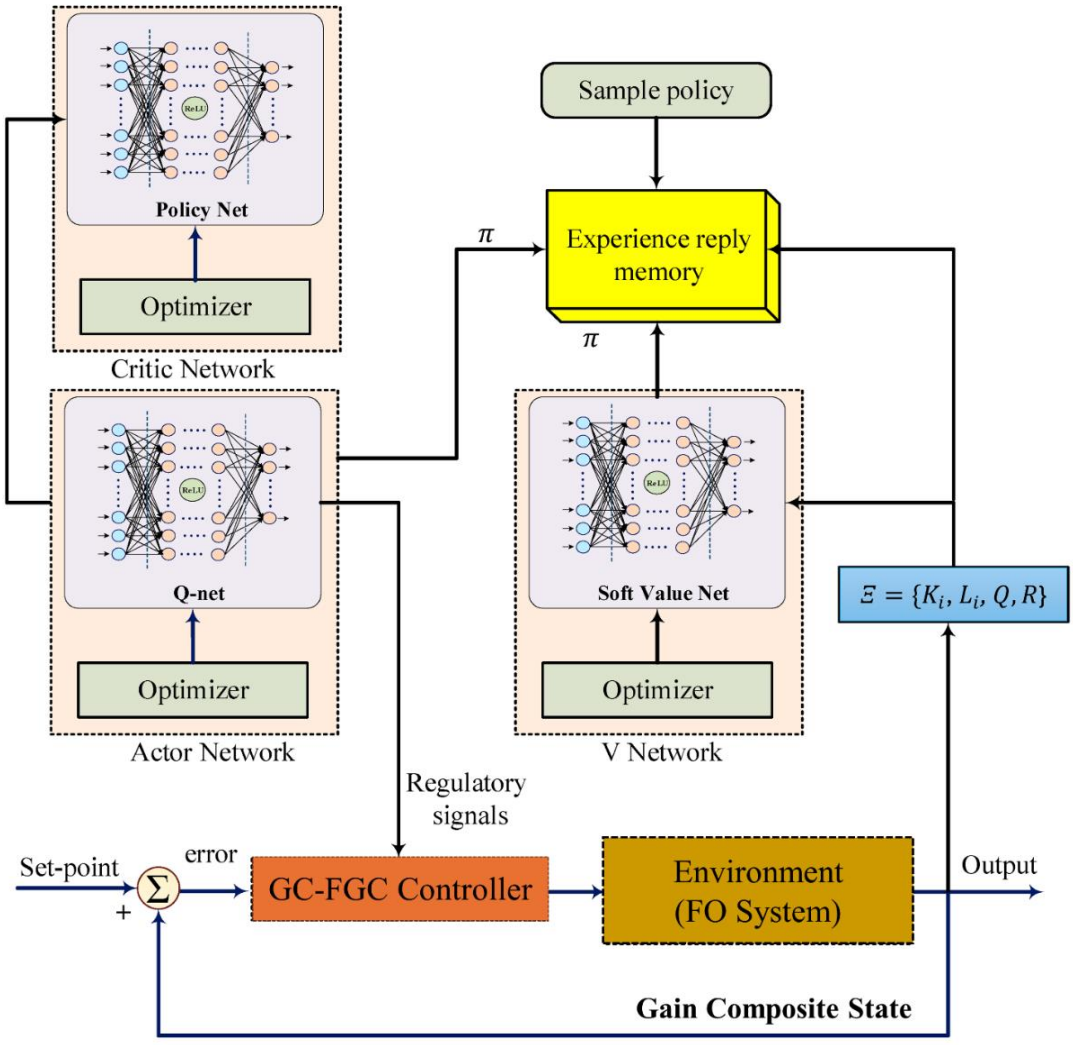

Figure 1. Architecture of GC-FGC controller utilizing SAC algorithm.

Table 1. Hyperparameter Settings for the SAC-Based Controller.

Parameter	Value	Parameter	Value
Actor network learning rate	10^{-3}	Discount-Factor (γ)	0.98
Critic network learning rate	10^{-4}	Activation-Function	Re-LU
Soft update coefficient (target smoothing)	5×10^{-3}	Batch-Size	2^8
Number of hidden layers per network	2	Mini-batch-Size	2^6
Neurons in first hidden layer	200 × 300	Optimizer	Adam

Remark 8. Compared with conventional TS fuzzy and guaranteed-cost controllers, the proposed Guaranteed-Cost Fuzzy Gain-Composite controller exhibits the following advantages:

1. It adaptively updates the fuzzy gains using the SAC learning mechanism, which enhances convergence speed and adaptability.
2. The guaranteed-cost framework ensures robustness and bounded performance under parameter uncertainties.
3. The integration of fuzzy logic and deep reinforcement learning reduces the conservatism of the control design while maintaining stability guarantees.

These features collectively contribute to a more flexible and high-performance control architecture suitable for complex nonlinear systems.

5. Simulation results

In this section, the effectiveness and practical implementation of the proposed T-S fuzzy control approach are demonstrated through two case studies involving FO chaotic systems. **Scenario 1** focuses on controlling a non-autonomous 3D fractional-order modified hybrid optical system (FO-MHOS), while **Scenario 2** addresses the regulation of a modified fractional-order laser chaotic system (FO Laser CS) to further validate the controller's performance. The numerical simulations are carried out using a recently developed algorithm introduced in [38,39], with a fixed time step of $h = 0.001$.

Remark 9. Section 5 presents numerical simulations on fractional-order optical and laser chaotic systems, illustrating the performance of the GC-FGC controller (Section 3) enhanced by SAC-based adaptive tuning (Section 4). The results validate the combined effect of the theoretical controller design and learning-assisted optimization, demonstrating robustness, convergence, and guaranteed-cost performance under uncertainties.

5.1. Scenario 1

A novel 3D fractional-order modified hybrid optical system (FO-MHOS) was proposed in, with its dynamics governed by

$$\begin{cases} D^{\alpha}x_1(t) = x_2(t), \\ D^{\alpha}x_2(t) = x_3(t), \\ D^{\alpha}x_3(t) = -0.35x_3(t) - x_2(t) + 0.6\,x_1(t)\big(1 - x_1^2(t)\big). \end{cases} \tag{5.1}$$

It was shown in [40] that for $\alpha \in (0.7,1.03)$, the system exhibits unpredictable chaotic behavior. By considering of $\alpha = 0.99$, $x_1 \in (-d, d)$, and $d = 15$, the membership functions of the fuzzy

model for the FO-MHOS (5.1) are calculated as

$$M_1\big(x_1(t)\big) = 0.5\left(1 + \frac{x_1(t)}{d}\right),\ M_2\big(x_1(t)\big) = 0.5\left(1 - \frac{x_1(t)}{d}\right).$$

Thus, the following fuzzy dynamics are obtained

- First Rule: If $x_1(t)$ is $M_1\big(x(t)\big)$, then $D^{\alpha}x(t) = (A_1 + \Delta A_1)x(t) + B_1u(t)$,
- Second Rule: If $x_1(t)$ is $M_2\big(x(t)\big)$, then $D^{\alpha}x(t) = (A_2 + \Delta A_2)x(t) + B_2u(t)$,

where $x(t) = [x_1(t), x_2(t), x_3(t)]^T$, $u(t) = [u_1(t), u_2(t), u_3(t)]^T$, A_1, and A_2 show the unknown parameters of the system. ΔA_1 and ΔA_2 are uncertainties of the system, and B_1 and B_2 are the input-gain-function of the system, which are defined as follows.

$$A_1 = \begin{pmatrix} 0 & 1 & 0 \\ 0 & 0 & 1 \\ b(1-d^2) & -1 & -a \end{pmatrix},\ \Delta A_1 = \begin{pmatrix} 0.1\,cos(3\,t) & 0 & 0.05\,sin(t) \\ 0.15\,cos(t) & 0.1\,cos(3\,t) & 0 \\ -0.1\,sin(t) & 0 & -0.15\,sin(2\,t) \end{pmatrix},$$

$$A_2 = \begin{pmatrix} 0 & 1 & 0 \\ 0 & 0 & 1 \\ \beta(d^2-1) & -1 & -\alpha \end{pmatrix},\ \Delta A_2 = \begin{pmatrix} 0.1\,cos(3\,t) & 0 & -0.05\,sin(t) \\ 0.15\,cos(t) & 0.1\,cos(3\,t) & 0 \\ 0.1\,sin(t) & 0 & -0.15\,sin(2\,t) \end{pmatrix}$$

$$B_1 = \begin{pmatrix} -0.0965 & 0.157 & 0.0142 \\ 0.0971 & 0.0485 & 0.0422 \\ 0.110 & -0.08 & 0.0916 \end{pmatrix},\ B_2 = \begin{pmatrix} 0.1265 & -0.157 & 0.0142 \\ 0.095 & 0.155 & 0.1422 \\ 0.081 & 0.18 & -0.0916 \end{pmatrix}.$$

Therefore, one obtains $h_i\big(z(t)\big)$ as follows:

$$h_1\big(z(t)\big) = M_1\big(x(t)\big) \times N_1\big(x(t)\big),\ h_2\big(x(t)\big) = M_2\big(x(t)\big) \times N_2\big(x(t)\big).$$

Here, $N_1\big(x(t)\big) = N_2\big(x(t)\big) = 1$.

Using theorem 2, the GC-FGC control gains are selected as $K = [3.567, 4.217, 2.54]$ and $L = [4.68, 5.48, 3.541]$. Additionally,

$Q = \begin{pmatrix} 0.1 & 0 & 0 \\ 0 & 0.1 & 0 \\ 0 & 0 & 0.1 \end{pmatrix}$ and $R = \begin{pmatrix} 0.1 & 0 & 0 \\ 0 & 0.1 & 0 \\ 0 & 0 & 0.1 \end{pmatrix}$ are given for cost function J and

$$\phi\big(u(t)\big) = \begin{cases} 0.5 & if\ u_i(t) > 0.5 \\ 0.97\,u_i(t) & if\ -0.5 \le u_i(t) \le 0.5 \\ -0.5 & if\ u_i(t) < -0.5 \end{cases} \quad i = 1, 2, 3 \tag{5.2}$$

To validate the stabilization performance of the FO-MHOS, represented by equation (5.1), the dynamic behavior under the proposed control scheme is illustrated in Figure 2. This figure demonstrates that the chaotic oscillations of the FO-MHOS are effectively attenuated over time, indicating the successful suppression of instability and the convergence of the system's trajectories toward equilibrium. The rapid decay of state variables signifies the controller's ability to dominate the inherent nonlinear dynamics of the FO-MHOS, achieving global stabilization.

Furthermore, the corresponding bounded GC-FGC control gains (5.2) employed to achieve this regulation are presented in Figure 3. These saturated control inputs (5.2) are subject to actuator

saturation constraints and are designed to maintain stability while respecting the physical limitations of real-world systems. As shown in Figure 3, the bounded GC-FGC control gains control signals (5.2) do not exhibit any chattering behavior, a common issue in discontinuous control methods such as conventional sliding mode control. The smooth and continuous nature of the control action suggests a well-designed control law that ensures robustness without introducing undesirable high-frequency oscillations.

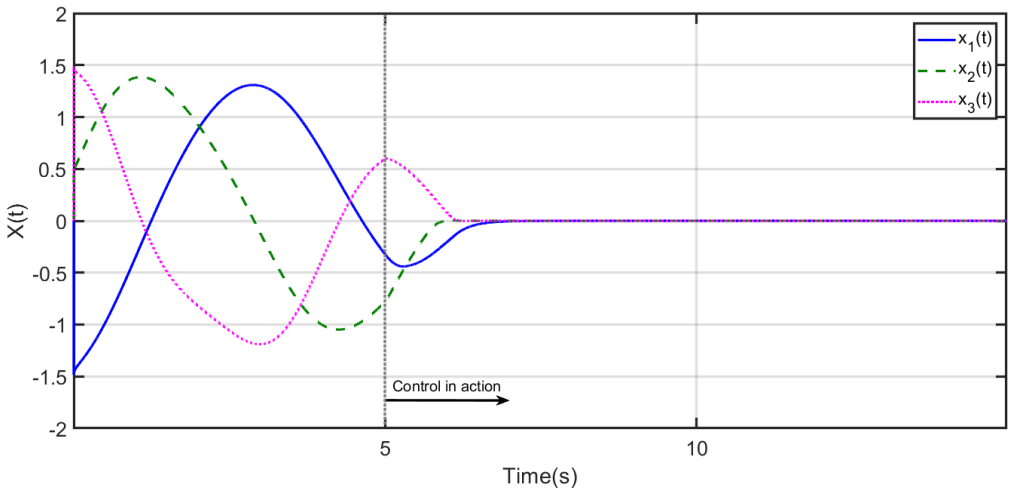

Figure 2. Stabilized attractors of the FO-MHOS (5.1) controlled with GC-FGC control signals (5.2).

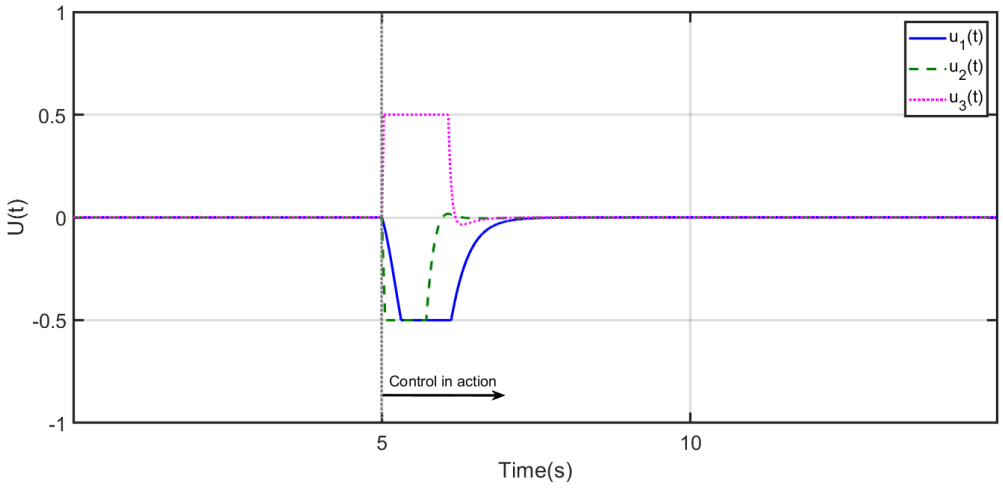

Figure 3. Saturated GC-FGC controller (5.2) to stabilize the FO-MHOS (5.1).

As the control signals approach their saturation thresholds, the imposed saturation function becomes active, effectively limiting their magnitude. This leads to the so-called "jumping phenomenon," where the system's behavior shifts between operating regimes. Such jump responses are not only tolerable but can be advantageous in practice, particularly in relay-based implementations or when hardware constraints necessitate saturation limits. These transitions between saturated and

unsaturated states resemble switching behavior, which can be deliberately exploited in hybrid or piecewise systems.

In addition, Figure 4 illustrates the trajectory of the cost function associated with the optimal control framework, as defined by equation (3.3). Over time, the cost function converges to a steady-state value, indicating that the controller not only stabilizes the system but also does so efficiently in terms of performance criteria such as energy expenditure or tracking precision.

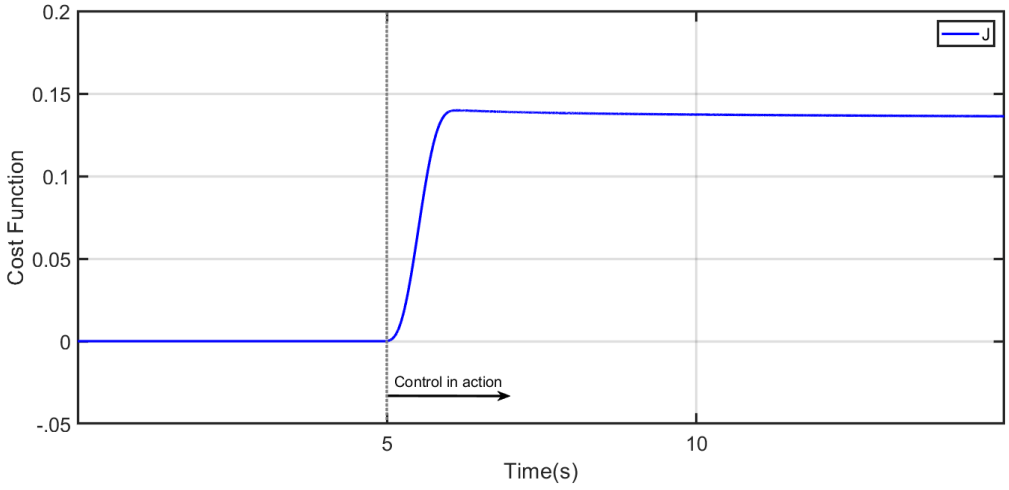

Figure 4. The FO Guaranteed-cost function (3.3) operated to stabilize the FO-MHOS (5.1).

Overall, the results confirm that the developed GC-FGC controller successfully stabilizes the FO-MHOS (5.1), ensuring robust performance while maintaining bounded control actions and avoiding chattering. The controller achieves this by combining fuzzy modeling, saturation-aware design, and finite-time convergence principles.

5.2. Scenario 2

Here, the effectiveness of the suggested GC-FGC control method (3.5) is shown by stabilization of the fractional-order laser chaotic system (FO Laser CS), which has chaotic behaviors for $\alpha = 0.97$ whose it's dynamics is given by [41,42]

$$\begin{aligned} D^{\alpha}x_1(t) &= 4\big(x_2(t) - x_1(t)\big) \\ D^{\alpha}x_2(t) &= -x_2(t) + 0.5x_3(t) + (27 + x_4(t))x_1(t) \\ D^{\alpha}x_3(t) &= \delta x_2(t) - x_3(t) \\ D^{\alpha}x_4(t) &= -1.8\, x_4(t) + x_1(t)x_2(t). \end{aligned} \tag{5.3}$$

Given the boundedness characteristics of the FO Laser CS (5.3), suppose that $x_2(t) \in [-d_1, d_1]$ and $x_4(t) \in [-d_2, d_2]$ where $d_1 = 20$ and $d_2 = 25$.

$$M_1\big(x_1(t)\big) = \frac{1}{2}\left(1 + \frac{x_1(t)}{d_1}\right), M_2\big(x_1(t)\big) = \frac{1}{2}\left(1 - \frac{x_1(t)}{d_1}\right),$$

$$N_1\big(x_2(t)\big) = \frac{1}{2}\left(1 + \frac{x_2(t)}{d_2}\right), N_2\big(x_2(t)\big) = \frac{1}{2}\left(1 - \frac{x_2(t)}{d_2}\right).$$

Thus, the following fuzzy dynamics are obtained

- First Rule: If $x_1(t)$ is $M_1\big(x(t)\big)$, then $D^\alpha x(t) = (A_1 + \Delta A_1)x(t) + B_1 u(t)$,
- Second Rule: If $x_1(t)$ is $M_2\big(x(t)\big)$, then $D^\alpha x(t) = (A_2 + \Delta A_2)x(t) + B_2 u(t)$,
- Third Rule: If $x_2(t)$ is $N_1\big(x(t)\big)$, then $D^\alpha x(t) = (A_3 + \Delta A_3)x(t) + B_3 u(t)$,
- Fourth Rule: If $x_2(t)$ is $N_2\big(x(t)\big)$, then $D^\alpha x(t) = (A_4 + \Delta A_4)x(t) + B_4 u(t)$,

where $x(t) = [x_1(t), x_2(t), x_3(t)]^T$, $u(t) = [u_1(t), u_2(t), u_3(t)]^T$, A_1, A_2, A_3, and A_4 are the unknown parameters of the system. ΔA_1, ΔA_2, ΔA_3, and ΔA_4 demonstrate uncertainties of the system, and B_1, B_2, B_3, and B_4 are the input-gain-function of the system, which are defined as follows:

$$A_1 = \begin{bmatrix} -4 & 4 & 0 & 0 \\ 52 & -1 & 0.5 & 0 \\ 0 & 0.5 & -1 & 0 \\ 0 & 0 & 0 & 1.8 \end{bmatrix}, A_2 = \begin{bmatrix} -4 & 4 & 0 & 0 \\ 2 & -1 & 0.5 & 0 \\ 0 & 0.5 & -1 & 0 \\ 0 & 0 & 0 & 1.8 \end{bmatrix},$$

$$A_3 = \begin{bmatrix} -4 & 4 & 0 & 0 \\ 27 & -1 & 0.5 & 0 \\ 0 & 0.5 & -1 & 0 \\ 20 & 0 & 0 & 1.8 \end{bmatrix}, A_4 = \begin{bmatrix} -4 & 4 & 0 & 0 \\ 27 & -1 & 0.5 & 0 \\ 0 & 0.5 & -1 & 0 \\ -20 & 0 & 0 & 1.8 \end{bmatrix},$$

$$\Delta A_1 = \begin{bmatrix} 0.1\,sin(t) & 0.15\,cos(2\,t) & 0 & 0.1\,sin(3\,t) \\ -0.1\,cos(3\,t) & 0 & 0.1\,sin(2\,t) & 0.2\,cos(2\,t) \\ 0 & 0.15\,cos(2\,t) & 0.15\,cos(2\,t) & -0.1\,cos(4\,t) \\ 0.1\,cos(t) & 0.1\,sin(t) & -0.1\,cos(4\,t) & 0 \end{bmatrix},$$

$$\Delta A_2 = \begin{bmatrix} 0.2\,sin(t) & 0 & 0.1\,sin(2\,t) & -0.1\,sin(3\,t) \\ -0.15\,cos(3\,t) & 0.2\,\sin(t) & 0 & 0.2\,cos(2\,t) \\ 0.1\,sin(t) & 0.1\,sin(2t) & -0.3\,cos(t) & 0 \\ 0 & 0.2\,sin(3t) & -0.1\,cos(4\,t) & 0.2\,sin(2\,t) \end{bmatrix},$$

$$\Delta A_3 = \begin{bmatrix} 0.1\,sin(t) & 0.15\,cos(2\,t) & 0.1\,sin(3\,t) & 0 \\ 0 & 0.1\,sin(t) & 0.1\,sin(2\,t) & 0.2\,cos(2\,t) \\ 0.1\,sin(t) & 0 & 0.15\,cos(2\,t) & -0.1\,cos(4\,t) \\ 0.1\,cos(t) & 0.1\,sin(t) & 0 & 0.1\,cos(4\,t) \end{bmatrix},$$

$$\Delta A_4 = \begin{bmatrix} 0 & 0.15\,cos(2\,t) & 0.1\,sin(t) & 0.1\,sin(3\,t) \\ -0.1\,cos(3\,t) & 0.1\,sin(t) & 0.1\,sin(2\,t) & 0 \\ 0.1\,sin(t) & 0.1\,sin(t) & 0 & -0.1\,cos(4\,t) \\ 0.1\,cos(t) & 0 & -0.1\,cos(4\,t) & 0.1\,cos(4\,t) \end{bmatrix},$$

$$B_1 = \begin{bmatrix} -0.165 & 0.157 & 0.0814 & 0.102 \\ 0.0971 & 0.0405 & -0.122 & 0.1485 \\ 0.110 & 0.08 & 0.0916 & 0.0387 \\ -0.095 & 0.157 & 0.0916 & -0.102 \end{bmatrix}, B_2 = \begin{bmatrix} 0.095 & 0.1095 & -0.204 & 0.141 \\ 0.273 & 0.351 & 0.092 & 0.251 \\ -0.18 & 0.132 & -0.616 & 0.487 \\ 0.195 & 0.157 & 0.1216 & 0.147 \end{bmatrix},$$

$$B_3 = \begin{bmatrix} 0.155 & 0.41 & -0.075 & 0.16 \\ 0.112 & 0.0885 & -0.270 & 0.152 \\ 0.110 & -0.08 & 0.0916 & 0.387 \\ -0.095 & 0.157 & 0.416 & 0.102 \end{bmatrix}, B_4 = \begin{bmatrix} 0.165 & -0.157 & 0.364 & 0.098 \\ 0.0971 & 0.325 & 0.412 & 0.188 \\ 0.1454 & -0.234 & 0.0916 & 0.047 \\ 0.095 & 0.671 & 0.34 & -0.129 \end{bmatrix}.$$

Therefore, we obtain membership functions of the fuzzy sets $h_i(z(t))$ as follows:

$$h_1(z(t)) = M_1(z(t)) \times N_1(z(t)),\ h_2(z(t)) = M_1(z(t)) \times N_2(z(t)),$$

$$h_3(z(t)) = M_2(z(t)) \times N_1(z(t)),\ h_4(z(t)) = M_2(z(t)) \times N_2(z(t)).$$

Based on theorem 2, the control gains are selected as $K = [4,4,4,4]$ and $L = [4,4,4,4]$. In addition, $Q = \begin{bmatrix} 0.19 & 0 & 0 & 0 \\ 0 & 0.11 & 0 & 0 \\ 0 & 0 & 0.41 & 0 \\ 0 & 0 & 0 & 0.22 \end{bmatrix}$ and $R = \begin{bmatrix} 0.13 & 0 & 0 & 0 \\ 0 & 0.12 & 0 & 0 \\ 0 & 0 & 0.15 & 0 \\ 0 & 0 & 0 & 0.1 \end{bmatrix}$ are given for cost function J and

$$\phi(u(t)) = \begin{cases} 10 & if\ u_i(t) > 10 \\ 0.95\, u_i(t) & if -10 \le u_i(t) \le 10 \\ -10 & if\ u_i(t) < -10 \end{cases} \quad i = 1,2,3. \tag{5.4}$$

The initial conditions of the system are selected as $x_1(0) = 5$, $x_2(0) = -2$, and $x_3(0) = 3$. To verify the stabilization capability of the proposed control framework for the 4D FO Laser CS, governed by Eq (5.3), Figure 5 presents the evolution of the system states under the applied control law. It is observed that the inherent chaotic oscillations of the FO laser system (5.3) are effectively suppressed, demonstrating the ability of the controller to drive the system trajectories toward the origin. This behavior confirms that the designed strategy is capable of managing the high-dimensional nonlinearities and memory-dependent dynamics that characterize fractional-order laser systems.

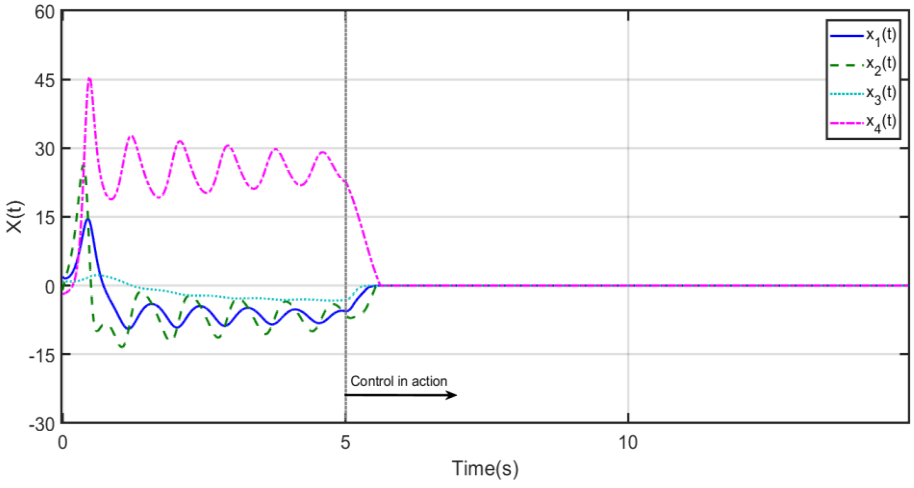

Figure 5. Stabilized attractors of the FO Laser CS (5.3) controlled with GC-FGC control signals (5.4).

The corresponding saturated control signals (5.4), responsible for achieving the desired stabilization, are depicted in Figure 6. These signals are subject to actuator limitations and are

implemented with a saturation function to ensure physical feasibility. The control profiles show a smooth response without any high-frequency chattering, which typically occurs in discontinuous or sliding mode-based control approaches. The absence of chattering highlights the robustness and practicality of the control law, which is essential for real-time implementation in optical and photonic systems where signal smoothness and stability are critical.

As illustrated in Figure 6, when the control signals (5.4) approach their saturation limits, the saturation function actively constrains their amplitude. In practical applications, such as semiconductor lasers or optical circuits, these bounded and switchable inputs are not only acceptable but often necessary to avoid damage to components.

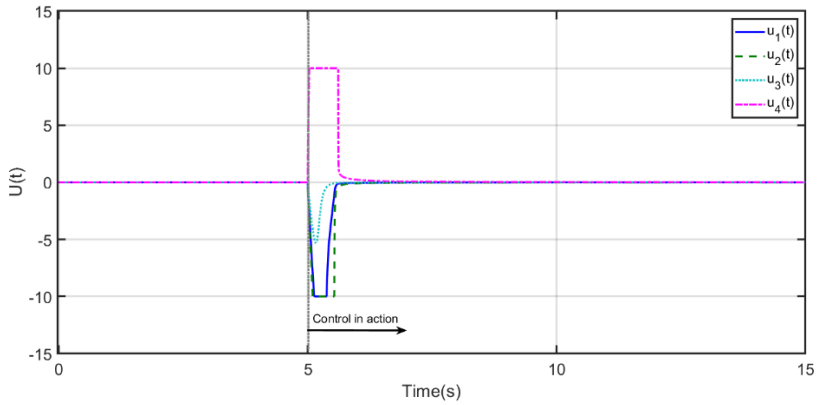

Figure 6. Saturated GC-FGC Controller (5.4) to stabilize the FO Laser CS (5.3).

Figure 7 further provides the evolution of the cost function defined in Eq (3.3), which measures the performance of the controller in terms of system regulation and control effort. The cost function exhibits convergence to a fixed minimal value, confirming that the control strategy achieves optimal performance as defined by the chosen criteria. This result indicates that the system has reached a stable state while minimizing energy consumption or control activity, a crucial requirement in laser applications where precision and efficiency are vital.

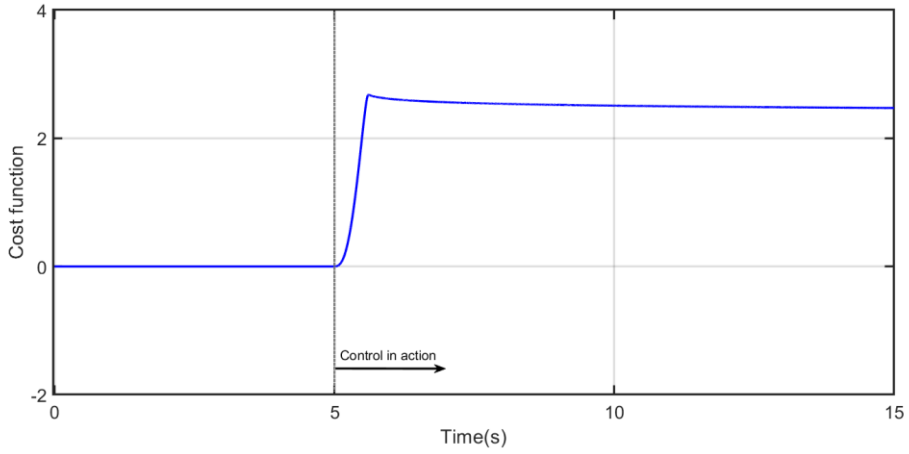

Figure 7. The FO Guaranteed-cost function (3.3) operated to stabilize the FO Laser CS (5.3).

To facilitate a comparative analysis, an adaptive fuzzy control (AFC) strategy is applied to stabilize the FO Laser CS described in (5.3) with $\alpha = 0.97$. This enables the performance of the AFC approach to be evaluated against the proposed GC-FGC control method (5.4) as well as other existing techniques. The researchers in [43] introduced an adaptive fuzzy controller specifically designed for the stabilization of fractional-order systems. The structure of this controller is summarized below:

$$u_i(t) = \begin{cases} -\left(5 + \bar{\xi}_i^{\,T}(t)\,\widehat{\varpi}_i\big(x_i(t)\big)\right) sgn\big(x_i(t)\big) - 5, \;\; x_i(t) > 0. \\ 0, \qquad\qquad\qquad\qquad x_i(t) = 0 \\ -\left(5 - \bar{\xi}_i^{\,T}(t)\,\widehat{\varpi}_i\big(x_i(t)\big)\right) sgn\big(x_i(t)\big) + 5, \;\; x_i(t) < 0. \end{cases} \tag{5.5}$$

$D^{0.98}\bar{\xi}_i(t) = 10|x_i(t)|\widehat{\varpi}_i\big(x_i(t)\big),\; i = 1, 2, 3, 4$.A comparative illustration of the controlled state trajectories of the FO Laser CS in (5.3) is shown in Figure 8.

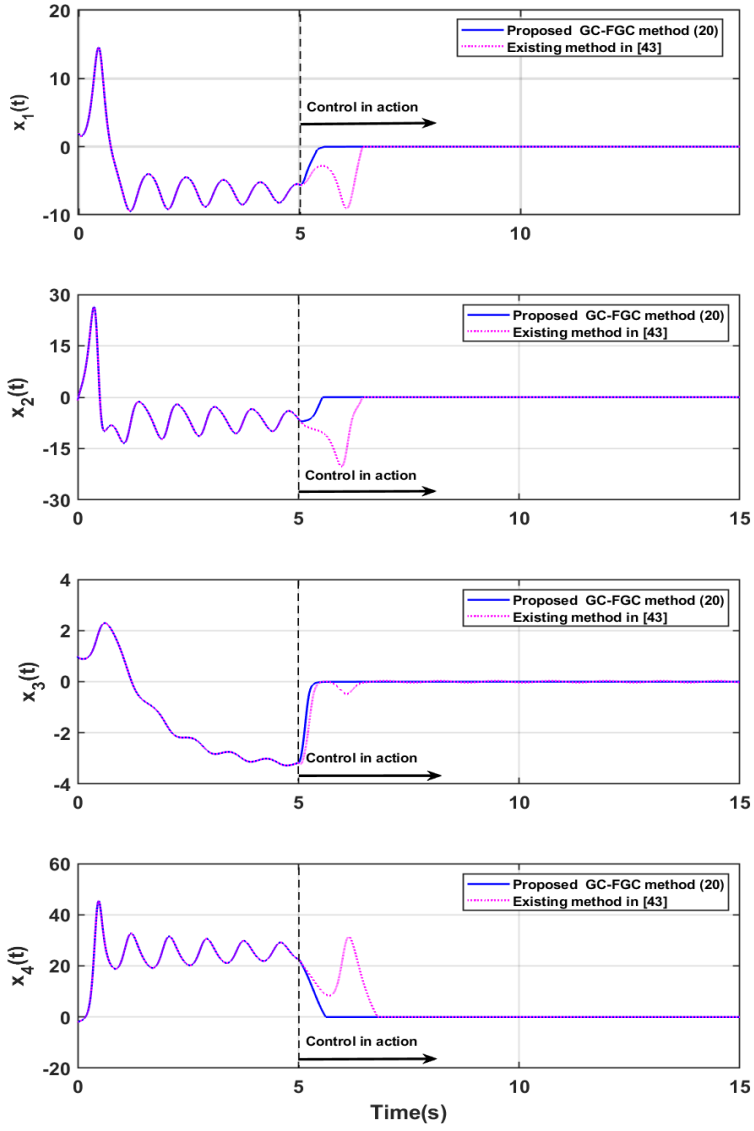

Figure 8. Comparison of the controlled variables $x_1, x_2,\; x_3$,and, $x_4$in the fractional-order chaotic FO Laser CS (5.3) using the proposed GC-FGC control method (5.4) and the AFC approach (5.5) described in [43] for $\alpha = 0.97$.

To regulate this system, both the AFC technique (5.5) and the proposed GC-FGC control strategy (5.4) are employed. While both controllers successfully drive the system states back to their equilibrium positions, the proposed GC-FGC method (5.4) exhibits a remarkably faster convergence speed and smoother transient response. The superior performance of the GC-FGC approach highlights its enhanced robustness and adaptability under system uncertainties and external disturbances. In contrast, the AFC technique (5.5) not only converges more slowly but also suffers from evident chattering effects, which are effectively eliminated by the proposed method. These results verify the efficiency and reliability of the GC-FGC controller as a significant improvement over existing approaches.

6. Conclusions

In this paper, a Guaranteed-Cost Fuzzy Gain-Composite control strategy was developed for the stabilization of a class of chaotic fractional-order (FO) T–S fuzzy nonlinear optical systems. The controller was designed based on the fractional-order Lyapunov stability framework and formulated using Linear Matrix Inequality conditions, ensuring asymptotic convergence of the system states despite the presence of chaotic dynamics, input saturation, and system uncertainties. The proposed control law is dynamic-free and structurally independent of the explicit nonlinear functions, relying instead on the norm-bounded characteristics of chaotic system states. To enhance performance and ensure optimal tuning, a deep reinforcement learning mechanism based on the Soft Actor-Critic algorithm was integrated into the controller design. This enabled automatic adjustment of the GC-FGC controller's internal parameters through policy optimization, ensuring that the sliding motion satisfies the finite-time reachability condition. Extensive numerical simulations and two detailed examples confirmed the effectiveness and robustness of the proposed methodology. The results demonstrate that the GC-FGC controller offers a promising solution for managing complex fractional-order optical systems, with potential applications in nonlinear optics, photonics, and secure communication technologies.

Appendix

In this appendix, the detailed proof of Lemma 1 is presented for completeness and reference.

Proof of Lemma 1.

Since $\left\|\sqrt{\varepsilon}X^T\pi \pm \frac{1}{\sqrt{\varepsilon}}\Xi(t)Y\pi\right\|^2 \geq 0$, then:

$\varepsilon\pi^T XX^T\pi \pm \pi^T Y^T\Xi^T(t)X^T X \pm \pi^T X\Xi(t)Y\pi + \frac{1}{\varepsilon}\pi^T Y^T\Xi^T(t)\Xi(t)\pi \geq 0$, which implies that

$$\pm Y^T\Xi^T(t)X^T \pm X\Xi(t)Y \leq \varepsilon YY^T + \frac{1}{\varepsilon}Y^T\Xi^T(t)\Xi(t)Y.$$

By observing that $\Xi^T(t)\cdot\Xi(t) \leq I$, the desired inequality can be derived.

Author contributions

Sepideh Nikfahm Khoubravan: Methodology, Software, formal analysis, visualization, writing original draft preparation; Saeed Mirzajani: Methodology, writing original draft preparation, supervision; Aghileh Heydari: Conceptualization, validation, writing review and editing original draft preparation; Majid Roohi: validation, Conceptualization, writing review and editing, investigation, resources, project administration, supervision. All authors have read and approved the final version of the manuscript for publication.

Conflict of interest

The authors state that the publishing of this work does not include any conflicts of interest for them.

Use of Generative-AI tools declaration

The authors used ChatGPT (OpenAI) only for minor language editing and improving the readability of some paragraphs, without any technical or analytical use.

References

1. S. Y. Nof, A. M. Weiner, G. J. Cheng, Laser and Photonic Systems: Design and Integration, Taylor & Francis, (2014).
2. C. He, Y. Shen, A. Forbes, Towards higher-dimensional structured light, *Light Sci. Appl.*, **11** (2022), 205. https://doi.org/10.1038/s41377-022-00897-3
3. M. S. Asl, M. Javidi, Numerical evaluation of order six for fractional differential equations: stability and convergency, *Bull. Belg. Math. Soc. Simon Stevin*, **26** (2019), 203–221.
4. A. A. Alikhanov, M. S. Asl, C. Huang, Stability analysis of a second-order difference scheme for the time-fractional mixed sub-diffusion and diffusion-wave equation, *Fract. Calc. Appl. Anal.*, **27** (2024), 102–123.
5. M. S. Asl, M. Javidi, An improved PC scheme for nonlinear fractional differential equations: Error and stability analysis, *J. Comput. Appl. Math.*, **324** (2017), 101–117.
6. M. Roohi, S. Mirzajani, A. R. Haghighi, A. Basse-O'Connor, Robust stabilization of fractional-order hybrid optical system using a single-input TS-fuzzy sliding mode control strategy with input nonlinearities, *AIMS Math.*, **9** (2024), 25879–25907. https://doi.org/10.3934/math.20241264
7. R. Shalaby, M. El-Hossainy, B. Abo-Zalam, T. A. Mahmoud, Optimal fractional-order PID controller based on fractional-order actor-critic algorithm, *Neural Comput. Appl.*, **35** (2023), 2347–2380. https://doi.org/10.1007/s00521-022-07710-7
8. M. Roohi, S. Mirzajani, A. Basse-O'Connor, A no-chatter single-input finite-time PID sliding mode control technique for stabilization of a class of 4D chaotic fractional-order laser systems, *Mathematics*, **11** (2023), 4463.
9. M. T. Vu, S. H. Kim, D. H. Pham, H. L. N. N. Thanh, V. H. Pham, M. Roohi, Adaptive dynamic programming-based intelligent finite-time flexible SMC for stabilizing fractional-order four-wing chaotic systems, *Mathematics*, **13** (2025), 2078.
10. M. Roohi, S. Mirzajani, A. R. Haghighi, A. Basse-O'Connor, Robust design of two-level non-integer SMC based on deep soft actor-critic for synchronization of chaotic fractional-order memristive neural networks, *Fractal Fract.*, **8** (2024), 548.
11. C. Chen, H. Wang, J. Li, Observer-based adaptive control for fractional-order strict-feedback nonlinear systems with state quantisation and input quantisation, *Int. J. Syst. Sci.*, (2025), 1–17.
12. A. Jajarmi, M. Akbarian, D. Baleanu, Analysis and backstepping control of a novel 4D fractional chaotic oscillator, *Math. Methods Appl. Sci.,* (2025), In press.
13. H. Zou, M. Wang, Enhanced sliding-mode control for tracking control of uncertain fractional-order nonlinear systems based on fuzzy logic systems, *Appl. Sci.*, **15** (2025), 4686. https://doi.org/10.3390/app15134686

14. S. Tong, M. Cui, Fuzzy adaptive predefined-time decentralized fault-tolerant control for fractional-order nonlinear large-scale systems with actuator faults, *IEEE Trans. Fuzzy Syst.,* **32** (2024), 1000–1012. https://doi.org/10.1109/TFUZZ.2023.3317014
15. A. Sharafian, H.Y. Naeem, I. Ullah, A. Ali, L. Qiu, X. Bai, Resilience to deception attacks in consensus tracking control of incommensurate fractional-order power systems via adaptive RBF neural network, *Expert Syst. Appl.* **211** (2025), 127763. https://doi.org/10.1016/j.eswa.2025.127763
16. S. Mirzajani, S. S. Moafimadani, M. Roohi, A new encryption algorithm utilizing DNA subsequence operations for color images, *Appl. Math.* **4** (2024), 1382–1403.
17. Z. Rasooli Berardehi, C. Zhang, M. Taheri, M. Roohi, M. H. Khooban, Implementation of T-S fuzzy approach for the synchronization and stabilization of non-integer-order complex systems with input saturation at a guaranteed cost, *Trans. Inst. Meas. Control,* **45** (2023), 2536–2553. https://doi.org/10.1177/01423312231155273
18. X. Fan, Z. Wang, A fuzzy Lyapunov function method to stability analysis of fractional-order T–S fuzzy systems, *IEEE Trans. Fuzzy Syst.*, **30** (2022), 2769–2776. https://doi.org/10.1109/TFUZZ.2021.3078289
19. Y. Hao, H. Liu, Z. Fang, Observer-based adaptive control for uncertain fractional-order T-S fuzzy systems with output disturbances, *Int. J. Fuzzy Syst.*, **26** (2024), 1783–1801. https://doi.org/10.1007/s40815-024-01703-5
20. Y. Mu, H. Zhang, Z. Gao, J. Zhang, A fuzzy Lyapunov function approach for fault estimation of T–S fuzzy fractional-order systems based on unknown input observer, *IEEE Trans. Syst., Man, Cybern. Syst.,***53** (2023), 1246–1255. https://doi.org/10.1109/TSMC.2022.3196502
21. Y. Hao, Z. Fang, H. Liu, Stabilization of delayed fractional-order T-S fuzzy systems with input saturations and system uncertainties, *Asian J. Control,* **26** (2024), 246–264.
22. X. Fan, Z. Wang, Event-triggered integral sliding mode control for fractional order T-S fuzzy systems via a fuzzy error function, *Int. J. Robust Nonlinear Control,* **31** (2021), 2491–2508.
23. P. Mahmoudabadi, M. Tavakoli-Kakhki, Tracking control with disturbance rejection of nonlinear fractional order fuzzy systems: Modified repetitive control approach, *Chaos Soliton. Fract.,* **150** (2021), 111142. https://doi.org/10.1016/j.chaos.2021.111142
24. R. Kavikumar, R. Sakthivel, O. M. Kwon, P. Selvaraj, Robust tracking control design for fractional-order interval type-2 fuzzy systems, *Nonlinear Dyn.*, **107** (2022), 3611–3628. https://doi.org/10.1007/s11071-021-07163-y
25. R. Elavarasi, G. Nagamani, Region bounded observer design for T-S fuzzy systems with nonlinear perturbations, *Commun. Nonlinear Sci. Numer. Simul.,* **151** (2025), 108998. https://doi.org/10.1016/j.cnsns.2025.108998
26. Y. Hao, Z. Fang, H. Liu, Adaptive T-S fuzzy synchronization for uncertain fractional-order chaotic systems with input saturation and disturbance, *Inf. Sci.,* **666** (2024), 120423. https://doi.org/10.1016/j.ins.2024.120423
27. K. Liu, W. Tang, Y. Sheng, Z. Zeng, N. R. Pal, Event-triggered finite-time stabilization of delayed T–S fuzzy systems on time scales, *IEEE Trans. Cybern.,* (2025), 1–10. https://doi.org/10.1109/TCYB.2025.3573795
28. J. Sun, Y. Yan, S. Yu, Adaptive fuzzy control for T-S fuzzy fractional order nonautonomous systems based on Q-learning, *IEEE Trans. Fuzzy Syst.,* **32** (2024), 388–397. https://doi.org/10.1109/TFUZZ.2023.3298812
29. G. Narayanan, S. Lee, S. Ahn, Optimal fractional fuzzy sliding-mode control for fractional-order fuzzy systems based on actor–critic reinforcement learning scheme, *J. Franklin Inst.,* **362** (2025), 107804. https://doi.org/10.1016/j.jfranklin.2025.107804

30. I. Podlubny, Fractional differential equations: an introduction to fractional derivatives, fractional differential equations, to methods of their solution and some of their applications, Academic Press (1998), Vol. 198.
31. T. Zhang, L. Xiong, Periodic motion for impulsive fractional functional differential equations with piecewise Caputo derivative, *Appl. Math. Lett.*, **101** (2020), 106072. https://doi.org/10.1016/j.aml.2019.106072
32. T. Zhang, Y. Li, Exponential Euler scheme of multi-delay Caputo–Fabrizio fractional-order differential equations, *Appl. Math. Lett.*, **124** (2022), 107709. https://doi.org/10.1016/j.aml.2021.107709
33. T. Zhang, Y. Li, Global exponential stability of discrete-time almost automorphic Caputo–Fabrizio BAM fuzzy neural networks via exponential Euler technique, *Knowl.-Based Syst.,* **246** (2022), 108675. https://doi.org/10.1016/j.knosys.2022.108675
34. C. Li, W. Deng, Remarks on fractional derivatives, *Appl. Math. Comput.*, **187** (2007), 777–784. https://doi.org/10.1016/j.amc.2006.08.163
35. Y. Li, Y. Chen, I. Podlubny, Mittag–Leffler stability of fractional order nonlinear dynamic systems, *Automatica*, **45** (2009), 1965–1969.
36. S. Boyd, L. El Ghaoui, E. Feron, V. Balakrishnan, Linear matrix inequalities in system and control theory, SIAM, (1994).
37. M. Haklidir, H. Temeltaş, Guided soft actor critic: A guided deep reinforcement learning approach for partially observable Markov decision processes, *IEEE Access,* **9** (2021), 159672–159683.
38. A. A. Alikhanov, P. Yadav, V. K. Singh, M. S. Asl, A high-order compact difference scheme for the multi-term time-fractional Sobolev-type convection-diffusion equation, *Comput. Appl. Math.,* **44** (2025), 115. https://doi.org/10.1007/s40314-024-03077-8
39. A. A. Alikhanov, M. S. Asl, D. Li, A novel explicit fast numerical scheme for the Cauchy problem for integro-differential equations with a difference kernel and its application, *Comput. Math. Appl.*, **175** (2024), 330–344. https://doi.org/10.1016/j.camwa.2024.10.016
40. M. S. Abdelouahab, N. E. Hamri, J. Wang, Hopf bifurcation and chaos in fractional-order modified hybrid optical system, *Nonlinear Dyn.,* **69** (2012), 275–284.
41. H. Natiq, M. R. M. Said, N. M. Al-Saidi, A. Kilicman, Dynamics and complexity of a new 4D chaotic laser system, *Entropy,* **21** (2019), 34.
42. F. Yang, J. Mou, C. Ma, Y. Cao, Dynamic analysis of an improper fractional-order laser chaotic system and its image encryption application, *Opt. Lasers Eng.,* **129** (2020), 106031. https://doi.org/10.1016/j.optlaseng.2020.106031
43. H. Liu, S. Li, H. Wang, Y. Sun, Adaptive fuzzy control for a class of unknown fractional-order neural networks subject to input nonlinearities and dead-zones, *Inf. Sci.,* **454–455** (2018), 30–45. https://doi.org/10.1016/j.ins.2018.04.069

AIMS Press